A semi-automated parallel parking system for passenger cars

J Pohl[1]*, **M Sethsson**[2], **P Degerman**[2], and **J Larsson**[2]
[1]Volvo Car Corporation, Gothenburg, Sweden
[2]Division of Fluid and Mechanical Engineering Systems, Department of Mechanical Engineering, Linköping University, Linköping, Sweden

The manuscript was received on 6 January 2005 and was accepted after revision for publication on 31 August 2005.

DOI: 10.1243/095440705X69650

Abstract: Car parking has been, and still is, a growing problem, with increasing vehicle sizes in the luxury segment as well as sport-utility vehicles. This is especially true when bearing in mind the confined parking spaces in parking lots and cities. While damage during parking generally does not cause any injury to the passengers, it is costly and annoying. Park assist systems are by no means new on the market, since passive systems which provide longitudinal guidance using ultrasonic distance sensors have been available on the market for a number of years.

The system presented is a semi-automated approach to parallel parking problems, as they frequently occur in European and Asian cities. The challenge during the development of this system was to have as few components as possible added to a standard vehicle, seeking reuse of many of the already built-in functionalities. The result is a system that leaves the longitudinal control of the vehicle to the driver but automates the steering process, and even stops the vehicle when the final parking position is reached.

Keywords: electric steering gear, ultrasonic distance sensors, functional architecture

1 INTRODUCTION

Passive parking assist systems were introduced to the market during the 1970s, and have since then increasingly gained in popularity. This is especially true for larger vehicles as well as sport-utility vehicles, which are parked in confined spaces such as downtown parking. The term passive system here relates to the customer function, rather than the sensor system, which in most cases is an array of ultrasonic distance sensors mounted in the front and/or rear bumpers. These sensors often have an opening angle of 50–70°, which results in a sensor array that can report obstacles in the field of view with a comparatively small number of sensors, but with low angular resolution. In other words, these sensors measure the distance to an obstacle but not the direction to the obstacle. The driver is then informed about the distance to the obstacle by an audible warning or signal. These systems are available for both front and rear end, and even aftermarket systems are available. Analogous systems for permanent mounted use within home garages are also on the market.

Combining these wide-angle sensors with high-resolution ultrasonic sensors or a video camera leads to another derivative of a parking aid system, where the system guides the driver into the parking space by giving detailed steering information. Examples of these kinds of system were recently presented by several vehicle manufacturers and suppliers on a prototype basis. Other systems to enhance parking, which already have been introduced to the Japanese market, use a moving video image with superimposed graphics providing the driver with a view of the required vehicle movement. These systems can normally be used for all kinds of parking manoeuvres where the parking space is indicated on the ground by clearly visible marking lines.

* *Corresponding author: Volvo Car Corporation, Vehicle Control 96260, PVH34, Gothenburg, SE-405 31, Sweden. email: jpohl12@volvocars.com*

Automated or semi-automated parking aid systems have been demonstrated by several car manufacturers. The vehicle manufacturer Toyota has launched their system [**1**] through the hybrid vehicle 'Prius'. It is a fully automated parking system, meaning that driver interaction is restricted to acceptance or rejection of the identified parking space. A number of issues may arise from such a system, especially from a product liability point of view, since the vehicle takes over the parking task from the driver. A solution to that problem could be to keep the driver in the loop and thereby ultimately responsible for the whole parking manoeuvre. The vehicle manufacturer BMW has shown a system [**2**] that assists the driver in the search for a suitable parking space and in the steering control during a rearward parking manoeuvre. However, the driver is still responsible for longitudinal control.

The system presented here builds on an electric power assisted steering gear (EPAS) in terms of actuator, where the steering wheel angle can be controlled. Furthermore, the possibility to request a brake torque from the brake system is required. In terms of sensors the scanning of the vehicle surrounding is done using three ultrasonic sensors with a rather small opening angle of 15°. Odometric information from the wheel speed sensors and distance measurement from the ultrasonic sensors is combined into knowledge of the detected parking space size and position in relation to the vehicle.

A schematic view of the parking procedure is shown in Fig. 1. It is worth mentioning that it is commonly accepted as good practice to drive by the space first and then park the car into the space in reverse. That behaviour is used here to identify the parking space. The system notifies the driver when a sufficiently large parking space is found, and asks to stop and gently reverse the vehicle as well as release the steering wheel. Control of the steering is taken care of by the system, which even informs the driver about the distance to the vehicle behind in order to give the driver the opportunity to stop. The brakes are actuated when the vehicle has reached its final parking position and in the case of a suddenly appearing object.

Given the actuators to manoeuvre the car in terms of steering and braking, the main work of this project has been to establish the reference signals for these actuators. This paper describes such a system and the possibilities that have been found from practical tests and implementation. The safety and reliability of the system have been major limiting factors for the work. In this way the project differs from other similar efforts found in robot motion control and path planning.

2 FUNCTION DEFINITION

In this section the sequence of system states is presented, and required definitions for object and parking space classification are given. The system state diagram is shown in Fig. 2. If the on/off switch is activated, the first transition from deactivated to activated takes place and the system enters the first substate, namely 'sensors activated'. The requirement for changing to the subsequent 'parking space accepted state' is an identified valid parking space. When the driver has changed gear in order to start reversing the vehicle, the next state transition is made, which activates the actual steering and brake control. In case of detected obstacles or driver

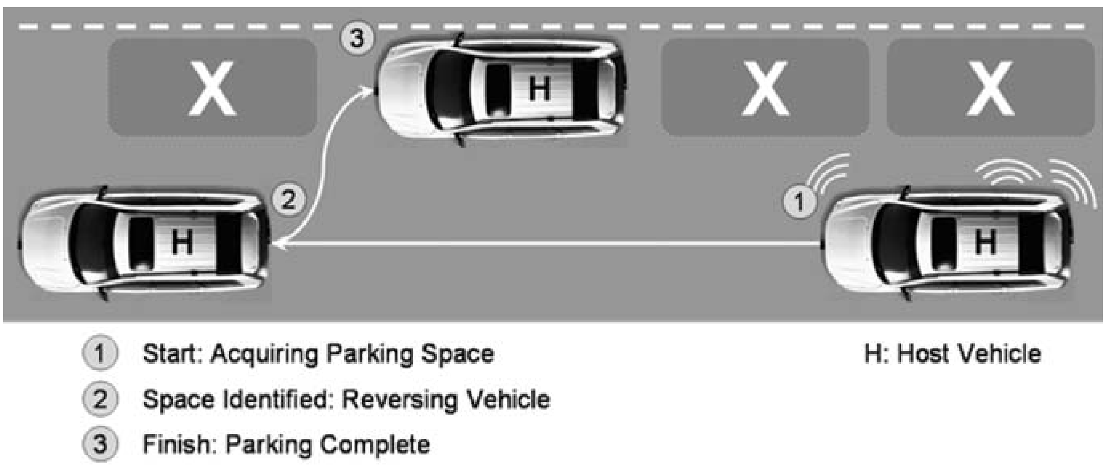

Fig. 1 Schematic view of a parallel parking manoeuvre, where the ultrasonic sensors capture the parking space dimensions and relative position to the car

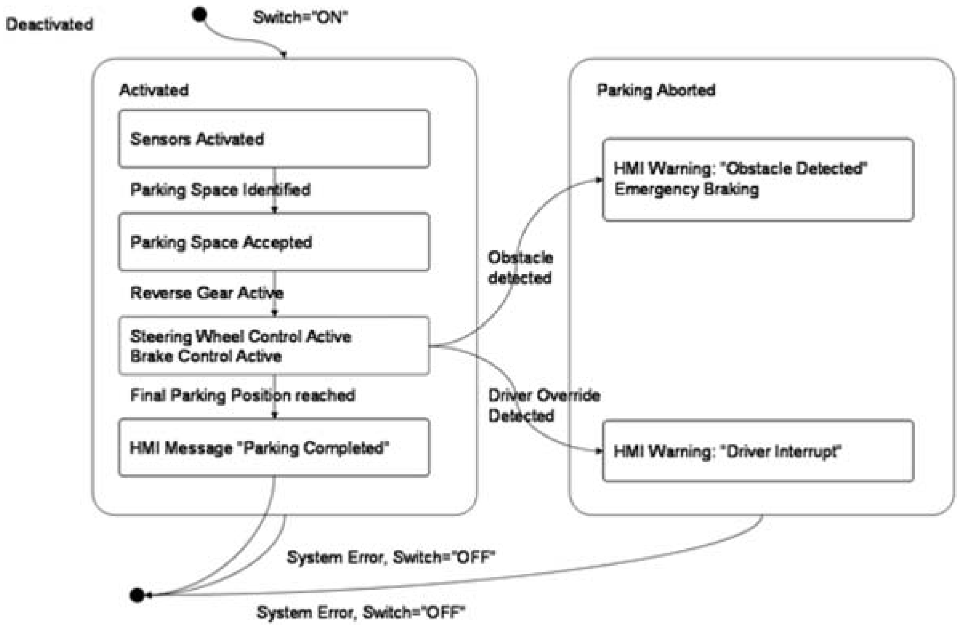

Fig. 2 State-space diagram of the automatic parking process

override condition, the 'parking aborted' state is entered and the vehicle is either stopped or the function is aborted. Criteria for what is called driver override are given in section 3. In the case where the final parking position detected condition is fulfilled, a text message is displayed to the driver. In Fig. 2, no state transitions due to timeout or overall system safety criteria are shown.

In order to classify a parking space as valid, the following requirements, or a combination thereof, must be fulfilled.

1. The space should have confining obstacles, such as other parked vehicles.
2. The space formed from these obstacles and the confining pavement curb or road curb should be square or nearly square.
3. The space should be at least as wide as the subject vehicle.
4. The space should allow for sufficient safety margins.

Otherwise the parking space will be classified as non-valid. Additional criteria for non-valid parking space are:

(a) detected valid obstacle within the parking envelope;
(b) required vehicle path not feasible with regard to current vehicle position.

Here, a valid obstacle is defined as an object or person prohibiting the completion of a started parking manoeuvre owing to:

(a) size (the vehicle does not fit into the parking space);
(b) other properties likely to cause damage to the vehicle;
(c) other properties likely to cause damage/injury to the obstacle/person.

The statements above make clear that the correct identification of a possible object within the parking envelope is decisive for the system function. However, a proper object classification cannot be guaranteed owing to the type of sensors used, i.e. a soft drinks can may result in the same sensor reading as, for instance, a pillar. From a failure means effect analysis (FMEA) point of view it is advantageous to receive assistance in object classification from the driver. Whenever the system receives a sensor reading indicating an object within the parking envelope, the driver is asked to confirm whether the obstacle is valid (according to the above definition) or not. Thereby the ultimate responsibility for both object classification and longitudinal vehicle control is left to the driver, which is preferable from a product liability perspective.

3 FUNCTIONAL ARCHITECTURE

In this section the functional architecture of the developed parking aid system as well as all involved function components is discussed in detail. The functional architecture consists of three major components, namely actuator system control (ASC), vehicle system control (VSC), and sensor system control (SSC), shown in Fig. 3. The VSC component itself is divided into different layers, namely driver, traffic, vehicle, and coordination layers.

An additional component is the human–machine interface (HMI) which consists of an activation button and an audiovisual display.

3.1 Sensor system control: ultrasonic sensor array

The task of the sensing system is to identify a suitable parking space within the vehicle surroundings. Several techniques may be used. Previously mentioned ones include ultrasonic range sensors and digital cameras, but also radar and electric field proximity sensors may be considered. The present work is based upon the use of ultrasonic sensors as these sensors are currently considered most suitable for serial production in passenger cars. This is due to robustness, cost, and installation requirements. The major difference between the sensors used and the ones employed in today's passive parking aid systems is the aperture size. With a larger sensor diameter, the opening angle and directional sensitivity become narrower. A typical opening angle lies in the range 15–20°. Typically, the wide-angle sensors have mounting diameters of about 8–12 mm and the more narrow sensors are in the range 45–55 mm. The design challenge here lies in finding a sensor installation that does not interfere with the overall visual appearance of the vehicle.

The sensors are triggered in sequence through an electronic signal and then fire an ultrasonic cone-shaped wavefront. The wavefront propagates forward and bounces off all obstacles it hits. The distance towards the detected obstacles is then calculated through the 'time-of-flight' principle. The narrow characteristic of the sensors has avoided 'cross-talk' effects on any sensor, in the case of which the sensors interfere with each other and thus produce unreliable measurements. However, a larger number of sensors may introduce such problems. Here, an array of three sensors per side was used.

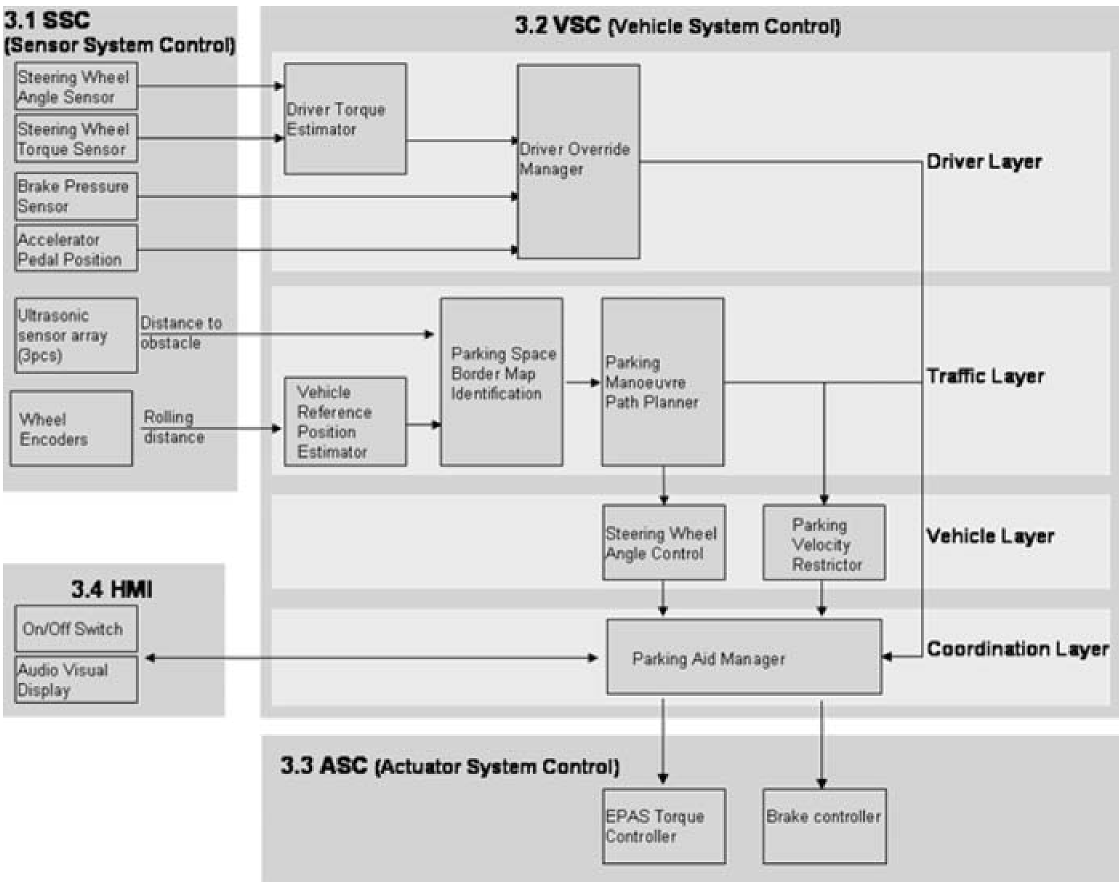

Fig. 3 Functional architecture of the parking aid system

3.1.1 Sensor data

Figure 4 shows a picture of the sensor. Its typical operational data are given in Table 1. The sensor is supposed to work under rather wet and harsh conditions. The sensor is of a combined type: the piezo-element is used both for sending and receiving. The required electronic driving circuit is integrated into the sensor and mounted on the back of the sensor element.

All sensors are interconnected through a specially developed differential signal interface system to ensure that the low-voltage TTL signals of the sensors are propagated correctly to the sensor array control computer. Using the TTL signals directly tended to introduce unreliable and noisy signals, mostly owing to interference from other electrical systems in the car. The cabling has to be capable of providing the 2 A of current needed during the ultrasonic transmission. The current drain is rather intermittent. It would be possible to decrease the requirements on the cabling using larger capacitors at the sensors. That is a question of mounting space for the sensors.

3.1.2 Sensor placement and operation

The placement of the sensors was studied in practical tests, and a number of different sensor configurations, from 3 to 6 sensors, were first tested on a prototype carriage. These tests were made with conventional vehicles on the university campus car parking lot as targets.

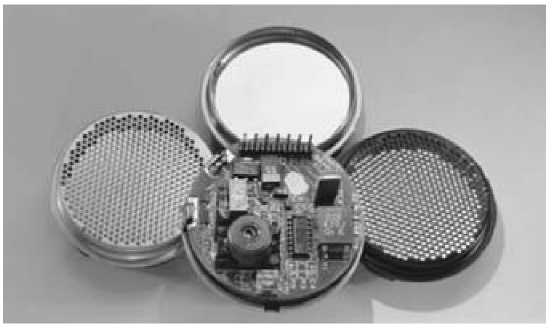

Fig. 4 Picture from the datasheet of the series 600 smart sensor of SensComp. Different front covers are shown. The grid front cover has a small influence on performance, but protects the sensitive surface of the piezomaterial

The placements of the sensors are dependent upon the criteria for valid obstacles. If the pavement is to be detected as a vital limiting border for the identified parking space, the sensors need to be slightly angled downwards (4–10°) to promote system sensitivity to obstacles on the ground. However, the parking space may also be constrained by other vehicles or walls. In that case it is better to have the sensor pointing straight outwards from the car. The chosen configuration uses both directions and has proved to be a good compromise of these two scenarios. A future arrangement of sensors will also be dependent on the mix of wide-angle and narrow-angle sensors, where the wide-angle sensors will be used to fulfil the requirements of close range as well as moving obstacle detection. The performance characteristics of the sensors were verified through simultaneous measurements using scanning laser distance equipment. In this way, sensor readings could be compared with measurements with a higher accuracy.

Special consideration was needed for the encapsulation of the electronics attached to the sensors. Moisture, vibration, and space requirements forced a redesign of the sensor mounting. A small plastic box was designed and the sensors were placed in that housing. A further study on temperature issues is needed, especially in applications during hot summer days in direct sunlight. The chosen sensor mounting positions are shown in Fig. 5.

The differential digital interface connects the sensors to a centrally embedded processor which controls the firing, sequencing, and time-of-flight measurements. The interface secures a well-defined trigger point in time. The overall sensor array system matches the accuracy specification of the sensors well, and no further information is lost during the sensor information fusion process. The time between wavefront and echo is measured by a 16 bit digital counter as commonly found in embedded processors. Using an 8 bit counter would have resulted in some information loss. The characteristics of the sensors may give some false readings for very close

Table 1 Ultrasonic sensor characteristics for the chosen ultrasonic sensor

Electrostatic transducer frequency	50 kHz
Beam angle	15° at -6 dB
Range	0.15–10 m
Absolute accuracy	± 1 per cent of true distance to object
Normal fire rate	5 Hz

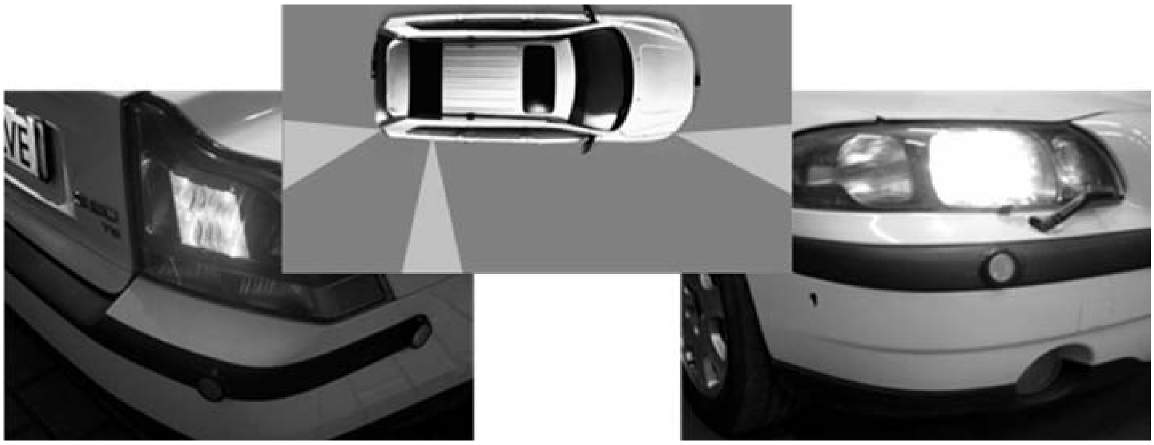

Fig. 5 During the test, sensors were only applied to the right side of the vehicle. They were placed at the rear right, front right, and right sideways. Initial tests were carried out using six sensors, but further studies showed that a smaller number of sensors is quite sufficient. As can be seen in the photos, the sensors have been mounted in a specially made ring in the bumper. The sensors have their central axis pointing out horizontally and slightly downward from the vehicle

obstacles. To avoid that, a small cancellation period was introduced, increasing the close-range limit to about 0.3 m.

3.1.3 Sensor limitations

The most severe limitation on the chosen sensors is operating temperature, which is guaranteed within the range 0–40 °C. The actual required measuring distance range is about 4–6 m; however, the sensors used here have an extensive range of up to 10 m. An adjustment to the required range may improve the accuracy and/or reduce the electric current consumption.

A common opinion about ultrasonic sensors in outdoor use is that they are sensitive to high-speed winds. No such problems were seen in this application, but further tests are still required, especially when it comes to the influence of strong winds on the overall parking performance of the system in terms of absolute position offset errors. The sensor performance in rain and snow conditions has still to be evaluated as well. The sonic signature from snowy cars and obstacles also needs to be studied.

3.2 Vehicle system control

3.2.1 Driver layer: driver torque detection and driver override manager

On account of product liability issues, it is advisable to keep the driver 'in the loop'. Thereby the driver ultimately is responsible for the safe control of the vehicle. In the semi-automated parking aid system presented here, this requirement is partly fulfilled through the driver's longitudinal control task. In other words, if the driver does not press the accelerator pedal, the vehicle will remain stationary. Another way of keeping the driver in the loop is through parking manoeuvre abortion due to detected adverse driver activity, or so-called driver override. A detected excessive driver torque during the parking manoeuvre will consequently abort the operation of the parking aid system. The idea behind this kind of driver override is similar to that in lane-keeping systems, where the driver's steering wheel torque is monitored in order to determine whether the driver is in the loop or not (see reference [**3**]).

The driver override must be intuitive, and therefore driver torque input to the steering wheel has been chosen as one driver override criterion. Others are accelerator pedal velocity and brake operation.

In order to estimate the driver torque, the existing steering column torque sensor of the EPAS system is used. If the torque applied on the steering wheel is understood as an outer disturbance, a Kalman filter including a simple model of the column assembly can be used. Such a Kalman filter requires a set of observable measurements; here, use is made of the pinion torque (as the torque sensor of the EPAS steering gear is used) and the steering wheel angle.

In Fig. 6, T_S represents the sensor torque, T_H represents the driver torque, $\hat{T}_H$ represents the estimated driver torque, L is the Kalman gain (calculated from the covariance matrices from process and measurement noise), B_V is the viscous friction coefficient, α is the steering wheel angle, and J is the steering wheel inertia. For real-time applications the filter needs to

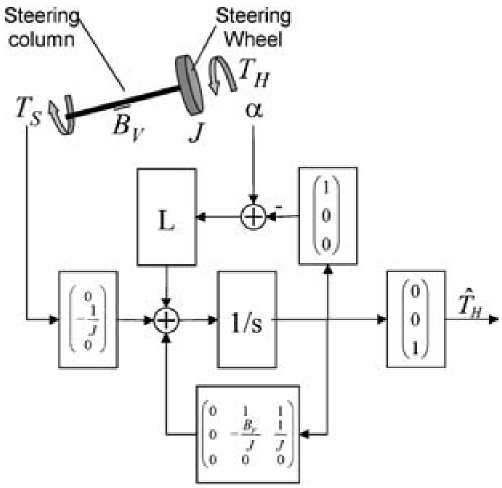

Fig. 6 Kalman filter as an observer of the outer disturbance T_{H}

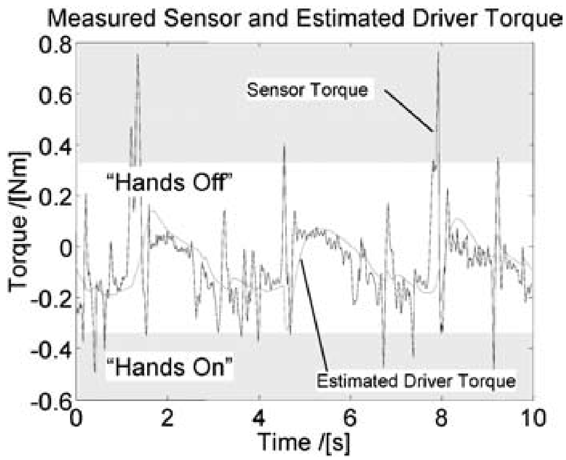

Fig. 7 Torque signals T_{H} and T_{S} of the steering column assembly from Fig. 6. The low-pass filter properties of the Kalman filter can clearly be seen

be transformed into the discrete time domain, which is straightforward using, for instance, the zero-order hold transform.

In situations where the driver does not apply any torque to the steering wheel, i.e. 'hands-off', the estimated driver torque $\hat{T}_{\mathrm{H}}$ should be zero if the model perfectly represents the dynamic characteristics of the steering column assembly. As, for example, frictional effects are only modelled by simple viscous friction and stick slip issues were neglected, the Kalman filter 'confuses' these with a torque from the driver. The same is true for acceleration effects (as well as gravity effects) due to a non-centric centre of gravity (CG), where the lateral acceleration (or gravity) times the steering wheel mass and CG eccentricity acts as a torque on the wheel. Acceleration effects are easy to implement into the filter but proved to have only a minor influence on the estimated steering wheel torque in contrast to non-linear friction.

However, thresholds can be used for deciding whether a given state represents 'hands-on' or 'hands-off' as a practical cure to the problem. If the observed driver torque is below a certain threshold over a certain time, the condition is classified as 'hands-off' (i.e. no driver intervention), otherwise a 'hands-on' condition is true which will deactivate the parking aid function. It is noticeable that the steering wheel is used in large movements during a normal parking manoeuvre. A 'hands-on' override situation will therefore result in a large input to the Kalman filter.

In Fig. 7 the measured and estimated sensor torque signals are shown, as well as two zones for 'hands-on' and 'hands-off' determination.

In a similar manner the brake system is utilized as an indicator for driver override detection: whenever a sudden increase in brake pressure owing to driver operation is detected, the system will enter the driver override state and abort the parking manoeuvre. Again, deciding whether the driver action is normal or panic braking is solved with a threshold value.

3.2.2 *Traffic layer: vehicle reference position estimator*

The vehicle reference position estimator function component consists of a vehicle model that computes the present car position, velocity, and angle given the encoder signals of both rear wheels. The output signals of this function component are the lateral and longitudinal distance of the centre of the rear axle, as well as the vehicle heading angle in relation to the starting position.

The wheel encoders provide 48 pulses per wheel revolution which gives a distance resolution of approximately 0.02 m in travelled distance for 225/45R16 tyres. This resolution is crucial for the change in vehicle angle, as this angle is calculated from the difference in travelled distance of the rear wheel sensors. However, with extrapolation where constant velocity is assumed between two subsequent pulses, the accuracy of the distance calculation increases, thereby improving vehicle angle calculation. This extrapolation has to be limited to the distance resolution, otherwise vehicle standstill cannot be correctly identified.

The present heading angle of the rear axle, denoted by α_{n+1} in Fig. 8, is the result of dividing the

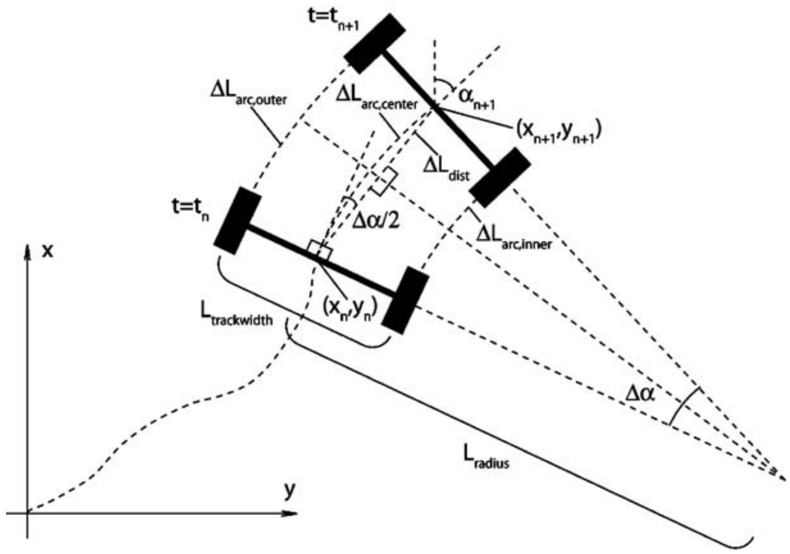

Fig. 8 Kinematic vehicle movement model (here the rear axles are shown at $t = t_n$ and $t = t_{n+1}$)

difference between the two accumulated rear wheel movements with $L_{\text{trackwidth}}$.

$$\alpha_{n+1} = \frac{\Delta L_{\text{arc,outer}} - \Delta L_{\text{arc,inner}}}{L_{\text{trackwidth}}} \tag{1}$$

The angle is measured relative to the fixed x axis. The current position is computed from the assumption that the car moves along an arc between the measurements, as in Fig. 8, where the rear axle of the vehicle is shown for two subsequent measurements at time t_n and t_{n+1}. Between the two subsequent measurements, the rear axle moves in a circle with radius L_{radius} over an angle $\Delta\alpha$. Below there follows a description of how to compute the updated position (x_{n+1}, y_{n+1}) given the position (x_n, y_n) one time step before, as well as an old and updated α.

The increment in heading angle is found from

$$\Delta\alpha = \alpha_{n+1} - \alpha_n \tag{2}$$

The lengths of the arcs $\Delta L_{\text{arc,outer}}$ and $\Delta L_{\text{arc,inner}}$ are known from the rear wheel encoders. Given these measurements, the radius of the movement is computed as

$$L_{\text{radius}} = \frac{\Delta L_{\text{arc,centre}}}{\Delta\alpha} = \frac{\Delta L_{\text{arc,outer}} + \Delta L_{\text{arc,inner}}}{2\Delta\alpha} \tag{3}$$

whereas basic trigonometry gives the distance ΔL_{dist} between the rear axle centres of the two measurements

$$\Delta L_{\text{dist}} = 2L_{\text{radius}} \sin\frac{\Delta\alpha}{2} \tag{4}$$

from which the new position (x_{n+1}, y_{n+1}) is computed

$$\begin{aligned} x_{n+1} &= x_n + \Delta L_{\text{dist}} \sin\left(\alpha_n + \frac{\Delta\alpha}{2}\right) \\ y_{n+1} &= y_n + \Delta L_{\text{dist}} \cos\left(\alpha_n + \frac{\Delta\alpha}{2}\right) \end{aligned} \tag{5}$$

Aggravating factors with the position estimation are changes in wheel radius and track width owing to car payload and tyre pressure. During straight driving, the quotient of the two-wheel radii can be adjusted, and, while parking, the ultrasonic sensors provide distances with which the absolute values of the radius are found.

3.2.3 *Traffic layer: parking space border map identification*

In the parking space border map identification, target vectors to the parking space corners are computed by combining distance data from the ultrasonic sensors with estimated car position and orientation from the previously described function component. This process of obtaining the parking space vectors can be described as follows.

As the vehicle moves along the potential parking spaces, the sensors are triggered and read. The sensor readings, i.e. the distances, are combined with the current vehicle position and result in an identified target point in the global coordinate system. The longer the distance to the target, the more inaccurate are the target point coordinates due to the sensor's aperture; i.e. the uncertainty of the target point increases with distance.

The measurement in Fig. 9 was started with the vehicle positioned at origin and stopped at the indicated location. Each arc-shaped line in the figure represents a measurement from one sensor. As the ultrasound moves within a cone-shaped area, the true readings lie somewhere between the arc boundaries. However, a reading can be caused by small, non-valid objects or by reflections of objects at other positions. A criterion for a valid sensor reading is therefore that the detected obstacle has to be detected at least twice, i.e. another sensor reading has an intersection with the current where the two arcs can be combined into a crossing point. Some discarded measurements are shown in the right part of the figure.

As measurements are collected, the function component estimates three lines that together form the parking space. The final lines are shown as thick horizontal lines in the figure. The first line goes alongside the car that is ahead of the parking space, the second line is the curb, if it exists, and the third line is alongside the car after the parking space. The lines are estimated by using the least-squares method where the vertical deviations between measurements and the line are minimized. The choice of which measurements to use for a certain line mainly depends on the position in the y direction. The curbside measurements should be quite a distance from the other measurements in the y direction.

When all constraining lines have been identified, the parking space corners are identified (numbered 1 to 4 in Fig. 9). The first corner is approximated by the last reading of the first line. The x coordinate of the second corner is chosen as the rightmost reading of the left car in Fig. 9, if such a reading exists, otherwise the x coordinate of the first reading of the curb line is chosen. The y coordinate of this corner becomes the y coordinate of the first reading of the curb line if the curb line exists. If a curb does not exist, the y coordinate is set to the y coordinate of the last reading of the first line plus the width of the host vehicle and a safety margin of 0.2 m. The third and fourth corners are approximated in a similar manner. When the corners are found, the parking space length, width, and position are calculated. If the parking space size is large enough for the host vehicle, the possibility to start the parking manoeuvre is communicated to the driver. If any stationary obstacles have been detected in the parking space, the driver is asked to confirm that the obstacle does not interfere with the parking manoeuvre. Dirt or small obstacles such as rubbish can give a similar reading as, for instance, a pole since the ultrasonic sensors do not detect the height of the obstacle.

The accuracy of the parking space estimation is limited by the lateral distance of the host vehicle to the parking space (owing to decreasing sensor resolution with increasing detection distance), as well as high host vehicle velocities (owing to fewer sensor readings per metre). If the host vehicle is driven far from the car parked ahead of the space and at high speed, the parking space length is estimated to be shorter than it is. This is due to the fact that the sensor pointing in the rearward direction may not have captured the front of the first parked car. The parking space estimation must then use a reading from the curbside, if available, or add a safety distance in the x direction.

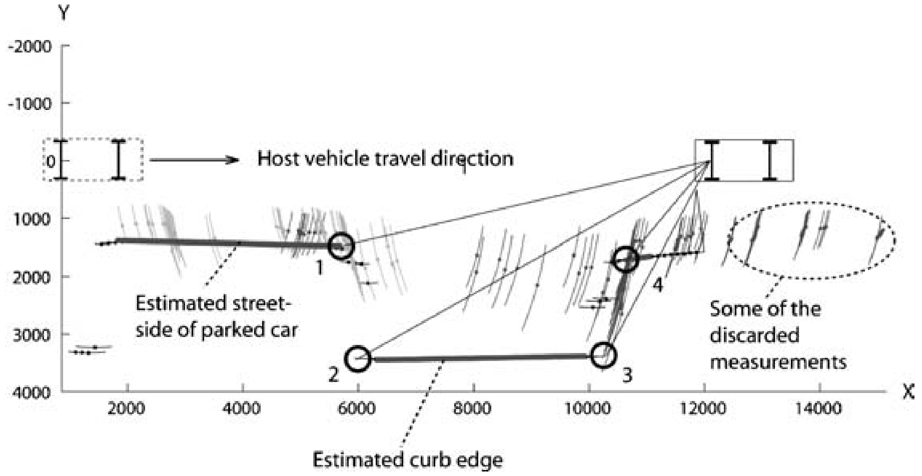

Fig. 9 Estimation of parking space position and size using ultrasonic sensors. The data come from measurement of a parking space between two cars parked parallel to a curb

3.2.4 *Traffic layer: parking manoeuvre path planner*

The parking manoeuvre path planner function component has two main objectives:

(a) to define a trajectory from the original position of the car into the parking space
(b) to compute a steering wheel angle request in order to make the rear axle centre follow it.

In this manner, the outputs of this function component are steering angle and brake pressure reference signals with which the car orientation and velocity are controlled relative to an identified parking space. A trajectory into a parking space can be defined in many ways, as has been shown, for instance, in references [**4**] to [**6**].

Here, the trajectory has three segments, as shown in Fig. 10. In the first phase the vehicle is reversed in parallel to the curb. In the second phase the inclined line shown in the figure is followed, and in the last phase the vehicle is turned to align with the curb. The advantages of this approach compared with skipping the straight line and performing the turns directly after another is that the vehicle will minimize its exposure to the traffic in the road.

In order to calculate the parking path, the geometry of both parking space and host vehicle is needed as well as safety margins.

Figure 11 illustrates the important geometry of parallel parking. The key position from which to calculate the path is shown, i.e. the position when the last turn is initiated to position the car parallel to the curb. The distances $L_{\text{marg,front}}$, $L_{\text{marg,side}}$, and $L_{\text{marg,curb}}$ are safety margins. The vehicle will thus always pass the car in front at a fixed distance. The lengths L_{back}, L_{side}, and L_{front} are given by the vehicle geometry itself, and the lengths $L_{\text{parkspace}}$ and L_{width} are computed from the identified parking space corners. The turning radius L_{radius} is determined by the maximum steering angle and vehicle wheel base. Now the angle ε of the path as well as the final distance to the rear vehicle, $L_{\text{marg,back}}$, can be computed as shown in equation (8)

$$\gamma = \arctan \frac{L_{\text{front}} + L_{\text{marg,front}}}{L_{\text{radius}} + L_{\text{side}} + L_{\text{marg,side}}} \tag{6}$$

$$\varepsilon + \gamma = \arccos \times \frac{L_{\text{radius}} + L_{\text{side}} + L_{\text{marg,curb}} - L_{\text{width}}}{\sqrt{(L_{\text{front}} + L_{\text{marg,front}})^2 + (L_{\text{radius}} + L_{\text{side}} + L_{\text{marg,side}})^2}} \tag{7}$$

$$L_{\text{marg,back}} = L_{\text{parkspace}} - L_{\text{back}} - (L_{\text{radius}} + L_{\text{side}} + L_{\text{marg,curb}} - L_{\text{width}}) \tan(\varepsilon + \gamma) \tag{8}$$

The angle ε also indicates when the final turn has to be initiated, and $L_{\text{marg,back}}$ shows whether the parking path is feasible ($L_{\text{marg,back}}$ should exceed a minimum safety margin).

3.2.5 *Vehicle layer: steering wheel angle request calculation*

The task is now to calculate the steering wheel angle request, $\delta_{\text{SteWhl,Req}}$, for the three sections of the parking manoeuvre as indicated in Fig. 10. During the first section the control target is to steer the vehicle parallel to the detected road curb. Prior to the first turning point, i.e. prior to the rear axle centre crossing the parking path, the control goal is to make the rear axle centre follow the parking path as accurately as possible. The steering wheel angle request is calculated in accordance with equation (9), where the steering wheel angle request is the sum of the angle error between vehicle angle and parking path angle, as well as the lateral offset towards the parking path

$$\delta_{\text{SteWhl,Req}} = k_\alpha(v)\, \alpha_{\text{err}} + k_{\text{e}}\, L_{\text{err}} \tag{9}$$

When the second turning point is approached, the vehicle is steered parallel to the curb as in the first

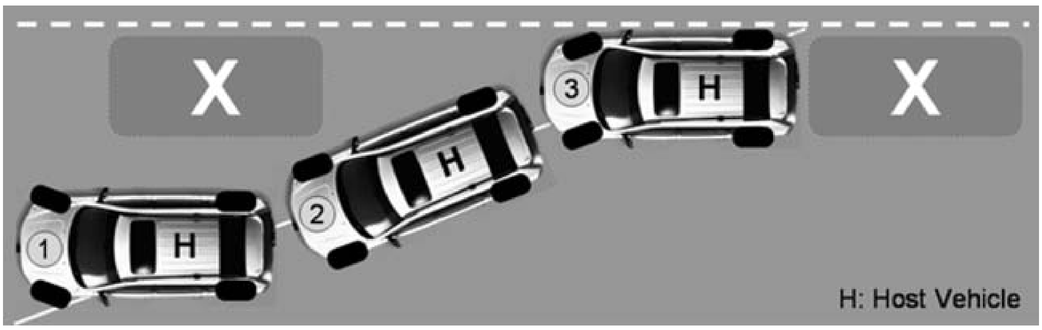

Fig. 10 Three segments of the parking procedure

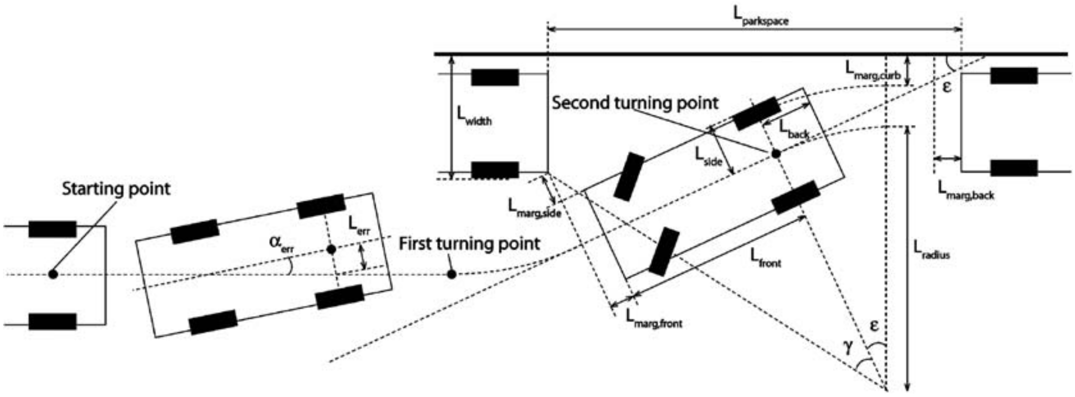

Fig. 11 Parking trajectory

section. The steering angle control request calculation has to take the limited actuation speed of the electric steering gear as well as the vehicle speed into account in order to estimate how much the request signal has to be advanced.

3.2.6 *Vehicle layer: parking speed limiter*

Velocity control, that is, constraining the vehicle velocity, is only required during the actual steering manoeuvre. Without a limited maximum speed, the requested steering wheel angle cannot be obtained with negligible longitudinal vehicle movement deviation. Constraining the vehicle velocity is therefore important, as the decision whether the particular parking space is sufficient depends on the subsequent vehicle speed.

The brake pressure command signal is computed from a proportional controller, using the allowed vehicle speed as a reference signal and the actual vehicle speed as feedback, provided that the current vehicle speed exceeds a speed threshold. Therefore, this is not really a velocity control but rather a speed limiter, as already indicated by the function component name. Before the first turning point, the reference velocity is set quite high to make the parking manoeuvre fast. As the vehicle approaches the second turning point, the speed threshold is gradually reduced in order to slow down the vehicle in time for the turn and avoid excessive vehicle speed. When the vehicle is parallel to the curb, a parking pressure is applied and the car stops.

3.2.7 *Coordination layer: parking aid manager*

The task of the safety manager is to guarantee a collision-free parking scenario. There are principally two different hazards that can endanger the successful completion of the manoeuvre, namely inner and outer hazards. Inner hazards are adverse driver behaviour, while outer hazards are changes in the environment, such as additional or newly detected obstacles.

Different actions have to be performed by the system, depending on the type of hazard detected. For outer hazards the system will go over to emergency braking in order to avoid or mitigate a collision. For inner hazards, such as driver intervention, the system will simply abort the parking manoeuvre. The difficulty lies in detecting internal and external hazards, and in finding a tuning suitable for all driver situations. Criteria for abortion of system operation in terms of adverse driver behaviour are:

(a) excessive detected steering wheel torque, i.e. the driver has not released the steering wheel;
(b) overspeed/overacceleration;
(c) excessive driver braking, i.e. emergency braking.

3.3 Actuator system control: EPAS torque controller

As mentioned earlier, the steering actuator control is a steering wheel angle control using the EPAS steering gear. As soon as the parking aid function is activated, a steering wheel angle controller is started, which calculates an additional EPAS motor torque that is superimposed on the assist torque.

The superimposed parking aid torque is calculated by

$$T_{\mathrm{SteWhl,Req}} = k_{\mathrm{P}}(\delta_{\mathrm{SteWhl,Req}} - \delta_{\mathrm{SteWhl}}) - k_{\mathrm{D}}\,\dot{\delta}_{\mathrm{SteWhl}} \tag{10}$$

which is a simple PD controller. Tuning of the controller can be done independently of the parking aid algorithm by using an artificial input signal such as a ramp or a sine function. The goal of the controller is to follow the reference angle $\delta_{\mathrm{SteWhl,Req}}$ without excessive overshoots, yet with as low a phase lag as possible. The controller parameters proved to be largely unaffected by varying operating conditions in terms of road surface.

3.4 Human–machine interface (HMI)

A method called 'scenario-based thinking' can be a substantial aid during both HMI synthesis and analysis phases.

1. The driver expresses a wish to park the vehicle by activating the system.
2. The sensor system becomes operational and identifies a potential parking space.
3. The driver is notified when a parking space of sufficient size and fulfilling all parking space criteria is found.

If the driver accepts the choice of parking space, the system enters the execution state of the parking manoeuvre by asking the driver gently to reverse the vehicle and activating the steering. The task of the HMI is to facilitate two-way communication as well as possible. During this work, the HMI has been developed in parallel with the sensor and control system. The driver operation of the system is essential to the design. A basic audiovisual interface has been incorporated into the test vehicle. The design of the user interface has presented a number of questions (these questions relate to the 'efficiency', 'safety', and 'learnability' criteria for HMI design, outlined in reference [**7**]).

1. What modality (auditory or visual, or a combination of both) should be used for the information presentation?
2. How much information does the driver need to complete an automatic parallel parking?
3. How should the interface be designed to be as safe in traffic as possible?

The HMI solution that was developed for the test vehicle was a screen presenting simple text messages to the driver: 'acquiring parking space', 'shift into reverse gear and release steering wheel and brake', 'parking in progress', and 'parking completed'.

For the HMI evaluation a group of 15 test participants (ten male and five female) was asked to perform car parking with the test vehicle, where an empty parking space was marked with cones. No other traffic was present. The test drivers were not given the possibility to familiarize themselves with the vehicle and the system prior to the test.

From these tests, the following conclusions can be drawn.

1. Drivers feel a need to intervene (i.e. control the vehicle velocity) during the reversing phase of the parking manoeuvre. The reason for this is that the test participants did not trust the system. Recommendations were to inform the driver more about the current system state in terms of planned path and current vehicle position through the display. Even a 'beep' sound was mentioned as a means to communicate the distance to the vehicle parked behind, as in conventional parking aid systems. Additionally, the wish was expressed to be allowed to use the brake, without cancelling the function, through a 'driver override manoeuvre'.
2. Two test participants mentioned the need to influence the parking manoeuvre by, for instance, two settings for the target distance between vehicle and curb. If the confining element is, for instance, a wall, it would be desirable to increase the target distance between vehicle and wall, so that the door can be opened.

4 RESULTS AND CONCLUSIONS

In terms of robustness the system has shown a highly repeatable performance under ideal conditions, which makes it particularly interesting to conduct robustness experiments under severe winter conditions. Severe winter conditions means here that the parking manoeuvres are carried out with summer tyres in slippery road conditions, and that the road curb itself is made up of a confining snow wall (see Fig. 12). The results of 30 consecutive runs are shown in Table 2.

In the present paper a semi-automated parallel parking system for passenger cars has been presented. Emphasis has been put on system integration issues such as a functional architecture and individual function components, which have been discussed in

Table 2 Mean value and standard deviation as well as the minimum and maximum values (all in cm) of the front/rear tyre distance to the curb and the distance to the rearward vehicle

	$L_{\mathrm{curb,front}}$	$L_{\mathrm{curb,rear}}$	L_{back}
Average	0.22	0.28	1.85
Standard deviation	0.05	0.06	0.10
Maximum	0.35	0.42	2.01
Minimum	0.10	0.17	1.62

Fig. 12 Winter conditions during a repeatability test with snow drift as the right-hand side parking space demarcation

detail. Human–machine interface issues were treated as an integral part of the system design, which led to an HMI solution that has been validated with a limited number of test drivers.

The main conclusions/results drawn from the work are as follows:

1. It is possible to use ultrasonic sensors to detect the surroundings of a car so that it can, with high repeatability even under harsh conditions, be guided into a parking space.
2. The sensors need to have a narrower aperture than the ultrasonic sensors used for passive parking aid systems.
3. The HMI has the task to inform the driver of current and future system actions in order to increase the driver's confidence in the system.

REFERENCES

1 Toyota launches all-new Prius, Toyota Corporate Information, Press Release, 2003, http://www.toyota.co.jp/en/news/03/0901a.html

2 BMW connected drive parking assistant, http://www.bmw.com/generic/com/en/fascination/technology/connecteddrive

3 **Pohl, J.** and **Ekmark, J.** Development of a haptic intervention system for unintended lane departure. SAE paper 2003-01-0282, 2003; *J. Passenger Cars – Electronic and Elect. Syst.*

4 **Xu, J., Chen, G.,** and **Xie, M.** Vision-guided automatic parking for smart car. In Proceedings of IEEE Intelligent Vehicles Symposium, Detroit, Michigan, 2000, pp. 725–730.

5 **Laugier, C.** Towards autonomous vehicles for future intelligent transportation systems. In Proceedings of Atti del Sesto Convegno della Associazione Italiana per *l'Intelligenza Artificiale*, Padova, Italy, 1998, pp. 251–258.

6 **Scheuer, A.** and **Fraichard, Th.** Collision-free and continuous-curvature path planning for car-like robots. In Proceedings of IEEE International Conference on *Robotics and Automation*, Albuquerque, New Mexico, 1997, pp. 997–1003.

7 **Preece, J., Rogers, Y.,** and **Sharp, H.** *Interaction design*, 2002 (John Wiley).

APPENDIX

Notation

B_V	viscous friction coefficient (N m/s)
J	steering wheel inertia (N m rad/s^2)
k_D	controller gain [N s/(m rad)]
k_e	controller gain (rad/m)
k_p	controller gain [N/(m rad)]
k_α	controller gain
L	various lengths (m)
L_{err}	distance control error (m)
L_{obs}	Kalman gain
s	Laplace operator ()
t	time (s)
T_H	driver torque (N m)
T_S	sensor torque (N m)
$T_{SteWhl,Req}$	requested steering column torque (N m)
$\hat{T}_H$	estimated driver torque (N m)
v	vehicle speed (m/s)
α	rear axle heading angle (rad)
α_{err}	angle control error (rad)
γ	second turning point to vehicle edge angle (rad)
δ_{SteWhl}	steering wheel angle (rad)
ε	parking path angle (rad)